

Poroelasticity is the dominant energy dissipation mechanism in cartilage at the nano-scale

+Tavakoli Nia, H.; Han, L; Li, Y; Ortiz, C.; Grodzinsky, A.
+Massachusetts Institute of Technology, Cambridge, MA
alg@mit.edu

INTRODUCTION: Recent studies of micro- and nano-scale mechanics of cartilage and chondrocyte pericellular matrix have begun to relate matrix molecular structure to its mechanical response [1,2]. AFM-based indentation has revealed rate-dependent stiffness at the micro-scale [1]. While multi-scale elastic behavior has been studied, and poroviscoelastic properties have been extensively documented at the tissue-level [3], time-dependent behavior and energy dissipation mechanisms of cartilage matrix at the nano-scale are not well understood. Here, we used AFM-based dynamic compression in conjunction with poroelastic finite element modeling to study the frequency-dependent behavior of cartilage using nano-scale oscillatory displacement amplitudes. We introduce the characteristic frequency f_{peak} at which the maximum energy dissipation occurs as an important parameter to characterize matrix time-dependent behavior. Use of micron-sized AFM probe tips with nano-scale oscillatory displacements over a 3-decade frequency range enabled clear identification of this characteristic frequency f_{peak} . The length-scale dependence of poroelastic behavior combined with judicious choice of probe tip geometry revealed flow-dependent and flow-independent behavior during matrix displacement amplitudes on the order of macromolecular dimensions and intermolecular pore-sizes.

METHODS Sample Preparation: Middle zone cartilage disks (9 mm diameter \times 0.5 mm thick) were harvested from the femoropatellar grooves of 1 – 2-week-old bovine calves and maintained in 0.154 M sterile phosphate buffered saline with protease inhibitors for less than 24 hours before testing. **AFM-Based Nano-indentation and dynamic compression:** Nano-indentation was performed using the MultiMode AFM with a PicoForce piezo and Nanoscope IV controller via the force mode (Veeco, Santa Barbara, CA). Gold-coated polystyrene colloidal probe tips (end radius, $R \sim 12.5 \mu\text{m}$, nominal spring constant $k \sim 4.0 \text{ N/m}$, Novascan Technologies, Ames, IA) were employed that were functionalized with a neutral hydroxyl-terminated self-assembled monolayer (OH-SAM, 11-mecaptoundecanol, Sigma-Aldrich, St. Louis, MO). The cantilever deflection sensitivity (nm/V) was calibrated on a hard mica surface, where the cantilever deflection equals the z-piezo displacement in the contact region. The thermal oscillation method was applied to determine the cantilever spring constant [4]. The piezo displacement profile was composed of indentation and force relaxation, followed by sinusoidal displacements over a frequency range $f = 0.3\text{--}130 \text{ Hz}$ (Fig. 1). The amplitude of the sinusoidal displacement, $\delta = 15 \text{ nm}$, was chosen to be much less than the initial indentation ($\delta \ll \delta_0$). Cyclic loading was applied following two different pre-indentation depths of $\delta_0 = 2.4 \mu\text{m}$ and $3.3 \mu\text{m}$, which correspond to the contact distances of $d = 7.9 \mu\text{m}$ and $9.3 \mu\text{m}$, respectively (Fig. 1). **Modeling:** was performed using the general purpose commercial finite element software ABAQUS (Version 6.9, SIMULIA, Providence, RI). Because of the symmetry of the problem, the specimen was modeled using axisymmetric, poroelastic elements. The spherical indenter was prescribed using a displacement history shown in the experiment of Fig. 1b. The indenter and the substrate surface were assumed to be rigid and impervious, and all other surfaces were assumed to be free draining. The dimension of the sample was set much larger than the radius of the indenter ($R \ll H, L$) to simulate an infinite domain for the width and depth of the sample. Both isotropic ($E = 0.1 \text{ MPa}$, $k = 2 \times 10^{15} \text{ m}^4/\text{N}\cdot\text{s}$, $\nu = 0.1$) and transversely isotropic models ($E_1 = E_3 = 5.8 \text{ MPa}$, $E_2 = 0.46 \text{ MPa}$, $\nu_{13} = \nu_{31} = 0$, $G_{12} = G_{23} = 0.37 \text{ MPa}$) (values taken from literature [5,6]) were used to simulate the dynamic behavior of the cartilage. The dynamic indentation modulus is defined as $E^* = f_{\text{osc}} / [2\delta (R\delta_0)^{1/2}]$ [7] (parameters defined in Fig. 1) and f_{osc} is the measured sinusoidal force amplitude. The angle ϕ is the measured phase lag between the force and applied displacement.

RESULTS: $|E^*|$ was found to asymptote at low frequencies at 0.09 MPa and 0.13 MPa for $\delta_0 = 2.4$ and $\delta_0 = 3.3 \mu\text{m}$, respectively. $|E^*|$ increased with frequency and began to level off near the frequency at which the phase lag was maximum. Upon further increases in frequency, $|E^*|$ plateaued at 0.6 MPa and 0.8 MPa for $\delta_0 = 2.4$ and $\delta_0 = 3.3 \mu\text{m}$, respectively. The phase lag between the force and displacement reached maxima at $f = 29.2$ and $f = 40.2 \text{ Hz}$ for $\delta_0 = 2.4$ and $\delta_0 = 3.3 \mu\text{m}$, respectively (Fig. 2b). Both the isotropic and transversely isotropic models predicted the same patterns for $|E^*|$ and ϕ vs. frequency as those observed experimentally. However, in the isotropic model the value of maximum

phase lag was $\phi_{\text{max}} = 8^\circ$, while in the transversely isotropic model the maximum phase lag varied with the choice of elastic constants. Both models predicted a shift in peak frequency of ϕ proportional to the inverse square of the contact distance, i.e., $f_{\text{peak}} \propto 1/d^2$. This prediction is in close agreement with the experimental peak frequencies of $f = 40.2$ and $f = 29.2 \text{ Hz}$, corresponding to the contact distances of $d = 7.9$ and $d = 9.3 \mu\text{m}$, respectively.

DISCUSSION: The measured phase lag (related to energy dissipation) during sinusoidal loading of cartilage over a 3-decade wide frequency range suggests that poroelastic dissipation is the dominant loss mechanism even at displacement amplitudes $\sim 15 \text{ nm}$ (e.g., compared to intrinsic matrix viscoelastic effects). This conclusion is supported by the observed shift in the phase lag peak frequency, f_{peak} caused by the change in indentation depth, δ_0 and the associated change in contact distance, d (Fig. 2), consistent with the trends predicted by the linear poroelastic prediction: $f_{\text{peak}} \propto 1/d^2$ (Fig. 3). Comparing the isotropic and transversely isotropic poroelasticity models (Fig. 3), it was found that the transversely isotropic model better predicted the range of changes in both the magnitude and phase lag of the dynamic modulus, as has been observed at the tissue scale [6,8]. Ongoing studies focus on a range of probe tip diameters to further explore the robustness of the approach, and parametric analysis using the theoretical model.

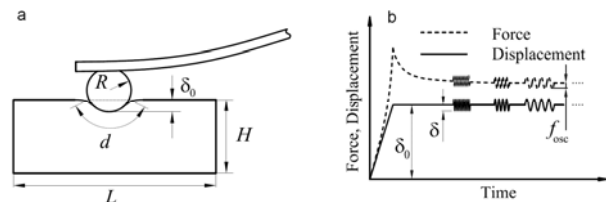


Fig. 1 (a) The geometry of the AFM-based dynamic compression experiment. (b) The applied displacement and resulting force profiles included a micro-scale pre-indentation and hold, and subsequent 15 nm amplitude sinusoidal compression at frequencies 0.3 – 130 Hz

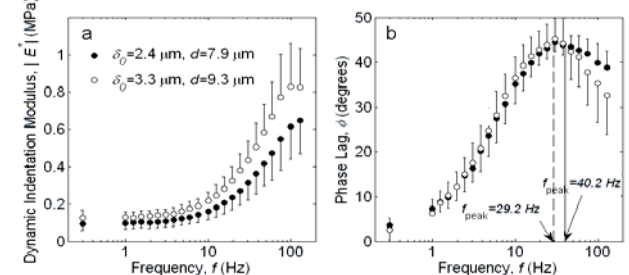


Fig. 2 Cartilage dynamic indentation modulus $|E^*|$ (a) and phase lag ϕ (b) at two pre-indentation depths $\delta_0 = 2.4$ and $3.3 \mu\text{m}$ (mean \pm SD, $n = 10$).

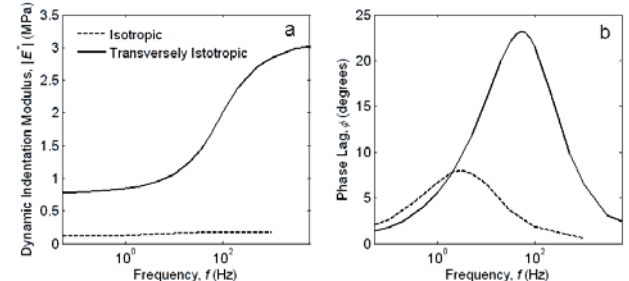


Fig. 3 Theoretically predicted dynamic indentation modulus (a) and phase lag (b) based on isotropic and transversely isotropic models.

REFERENCES: [1] Loparic+, *Biophys J* 2010 [2] Lee+ *J Biomechanics* 2010 [3] Ateshian *J Biomechanics* 2004 [4] Hutter+, *Rev Sci Instru* 1993 [5] Jurvelin *J biomechanics* 1997 [6] Cohen+ *J biomech Eng* 1998 [7] Mahaffy+, *Biophys J* 2004 [8] Soulhat+ *J. Biomech. Eng* 1999

ACKNOWLEDGMENTS: Supported by NSF Grant CMMI-0758651 and NIH-NIAMS Grant AR33236.